Advances in Computational Design, *Vol. 4, No. 3 (2019) 239-250*
DOI: https://doi.org/10.12989/acd.2019.4.3.239

Effects of temperature on the evolution of stresses at the stem cement interface

Djafar Ait Kaci, Abdelmadjid Moulgada*, Habib Achache and Noureddine Bounoua

Laboratory of Physics and Mechanical Materials (LMPM), University Djillali Liabes of Sidi Bel Abbes, Algeria

(Received September 25, 2018, Revised February 24, 2019, Accepted March 4, 2019)

Abstract. The insertion of femoral implants is the most important phase for surgeons, given the characteristics of the cement during its mixing phase, generating residual stresses of thermal origin that increase the different stresses induced in the bone cement. The aim of our study is to determine the different stresses that affect the cement and more particularly at the cement-implant interface for different temperatures, and to make a comparison with the cement at ambient temperature. It was concluded that, there are a large concentration of stresses in the proximal part of the cement. For normal stresses, the bone cement is affected by stresses of tension and compression due to the effect of polymerization and the contraction of the cement.

Keywords: temperature; polymerization; stem–cement interface; stresses

1. Introduction

In orthopedic surgery and particularly in the total hip arthroplasty, Perez *et al*. (2006) declare that the stem fixation is generally performed using a surgical cement, which consists essentially of polymer polymethyl-methacrylate (PMMA). According to Belkoff *et al*. (2003), the bone cement begins curing at a rapid rate immediately after the liquid monomers and the powder polymers are mixed. Baroud *et al*. (2004) showed that a crucial time frame exists in which the cement has the ideal viscosity for a successful injection, and a surgeon can miss this short handling window. Using a thermoelastic analysis, (Ahmed 1982, Ricker 2008) concluded that transient and residual stresses varied with different boundary conditions (temperature and adhesion at interfaces). Ahmed *et al*. (1982a) in their axisymetric model, measure the evolution of the temperature during polymerization in several places. The maximum values reached at the bone/ cement interface in the center of the thickness of the cement at the interface and stem-cement are quite high and are 90°C, 95°C and 110°C, due to the composition of the mixture (chemical reactions). The results of Iesaka *et al*. (2004) show a variation of the maximum polymerization temperature at the bone-cement interface between 48°C and 54°C depending on the initial temperature of the rod. However, these values appear to be very low compared to previous values. The digital simulations of Li *et* al. (2004) estimate maximal temperatures at the bone-cement interface according to the initial temperature of the stalk and the cement between 43°C and 65°C. Ahmed *et al*. (1982a) added that at the end of the process, when the bone cement polymerizes in contact with the cortical

*Corresponding author, Ph.D., E-mail: amoulgada@hotmail.fr

http://www.techno-press.org/?journal=acd&subpage=7 ISSN: 2383-8477 (Print), 2466-0523 (Online)

bone, which has impermeable surfaces, the residual radial stresses always remain compressive at the stem-cement interface due to the cement expansion. Serbetci 2004, Tunney and Hong (2007), Ricker 2008, and Gillani (2010) have reported improvement in the biological, thermal, and mechanical properties of PMMA bone cement after incorporating various types of additive particles (AP) into the cement. After their experience, Lai and Tai (2012) concluded that the average liquid time, paste time, and handling time were respectively 5.1 ± 0.7min, 3.4 ± 0.3min, and 8.5 ± 0.8 min. Hypothermic manipulation of bone cement is expected to reduce reaction rate and hence, extending the handling time. However, in a manner of reducing the environmental temperature of bone cement, Tai and Chen (2014) investigated that there are still uncertainties on handling time; cement distribution pattern and injection permeability of cement. The temperature of the mixing vessels should also be controlled. In addition, Benbarek *et al*. (2014) prove that the surgeon has no control over the industrial mixture of the components of the bone cement, which can vary considerably from batch to batch. Whitehouse *et al*. (2014) investigated that after the fixation of the implant, the thermal regression may weaken the bonding between bone and cement and contribute towards aseptic loosening, the most common cause of failure of THR. Baker *et al*. (2011) noticed that our instruments were often too hot to touch after preparing the femoral head for resurfacing, and questioned whether the heat generated could exceed temperatures. Gundapaneni *et al*. (2014) have proved that during implantation, bone cement undergoes a polymerization reaction, which is an exothermic reaction and results in the release of heat to the surrounding bone tissue. Janssen *et al*. (2012) after their study, the current findings suggest a potential thermal drawback of thick cement mantles, although it is unclear whether thermal bone necrosis significantly affects implant fixation or increases the fracture risk. Gergely *et al*. (2016) added that the optimum preparation procedures should keep cement and metal components at room temperature prior to mixing with a vacuum mixing system. Reducing cement mantle thickness may also be advantageous, as it reduces the maximum temperature and the risk of tissue damage.

The aim of this study is to analyse the effect of residual thermal stresses at the stem-cement interface on the mechanical behaviour of the Ceraver-Osteal model of cemented total hip arthroplasty by the computation of the stress distribution in the cement mantle. In this regard, the stress field in the bone cement is analysed statically by selecting the peak load during the walking activity of the patient. Two quantitative measures are calculated: stress distribution in the cement for different temperatures and make a graphical analysis for different stress according to the normalised distance for different component of THP at the cement-implant interface for different temperatures. It has been shown that each measure may lead to differing conclusions.

2. Materials and methods

2.1 Model designs

For a three-dimensional solid model of the total hip replacement (THR), there are four major components that have to be modelled: cortical bone, cancellous bone, femoral stem and cement. The complete models were assembled using Solidworks. The three-dimensional solid model assembly of femur, bone-cement and implant was transferred to Abaqus Workbench by the direct interface. Abaqus Workbench automatically recognizes the contacts existing between each part and establishes the contact conditions for corresponding contact surfaces.In this work, the Cevever-Osteal model of the cemented total hip arthroplasty is designed (Fig. 2).

Fig. 1 Steel Femur Stem

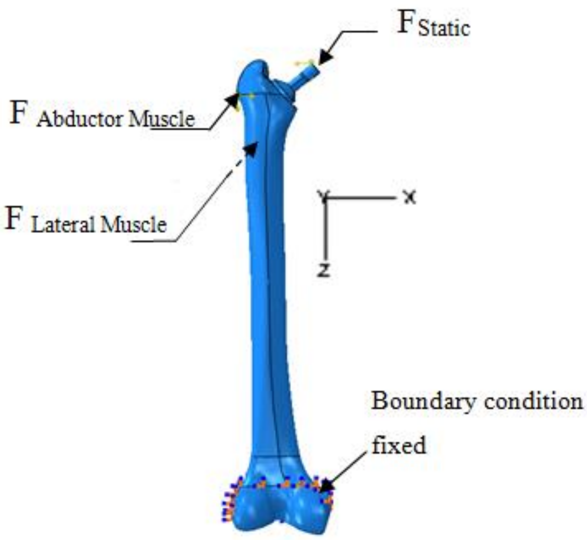

Fig. 2 Applied forces on the bone-cement–prosthesis assembly

2.2. Material properties

The material properties adopted were specified in terms of Young's modulus and Poisson's ratio for the implants and all associated components (Table 1). All materials were assumed to exhibit linear, homogeneous elastic behaviour by (Stolk 2007, and Benbarek 2014).

2.3. Loading and Boundary conditions

In this study, the load is applied on the surface of the implant bearing as shown in Fig. 2. Static load represents a person of 70 kg (Table 2), this load analysis is based, on the peak load during

Table 1 artificial hip components material properties according to Nuño (2002)

Materials	Young's modulus E (MPa)	Poisson ratioν
Cortical bone	15500	0.28
Concelleous bone	389	0.3
Stem (Ti-6Al4V)	110 000	0.3
Cement PMMA	2700	0.35

Table 2 Maximum loading configurations of the major muscles according to Lai and Tai (2012)

Load (N)	F_X	F_Y	F_Z
Joint contact force (Fstatic)	-433.8	-263.8	-1841.3
Abductor muscle	465.9	34.5	695.0
Lateral muscle	-7.2	-148.6	-746.3

normal walking activity. An abductor muscle load is applied to the proximal area of the greater trochanter. Lai and Tai (2012) have concluded that an ilio tibial-tract load is applied to the bottom of the femur in the longitudinal femur direction. Tai and Chen (2014) have proposed as the boundary condition is applied by fixing the distal epiphysis, which is the distal end of the femur that is connected to the knee. The coordinate system used to represent the direction of the forces components is shown in Fig. 2. The femur is primarily loaded in bending. Ahmed et al. (1982a) considered that the bone cement and the implant with respective thermal expansion coefficients 4.5x 10^{-5} °C^{-1} and 8.6x 10^{-6} °C^{-1}, the implant is maintained at an ambient temperature of 25°C, the cortical bone with a temperature of the human body of 37°C; during the cooling of the cement, the temperatures vary from 90 °C to 40°C.

2.4 Model Mesh

Finite element analysis (FEA) is a widely used research tool in biomechanics. The model in this study is discretized by using tetrahedral elements. This is because the geometry of the femur is irregular. Tetrahedral elements are better suited to curved boundaries compared to others elements. Discretizing by using tetrahedral elements with four nodes makes the meshing easier. The complete Osteal model (stem, bone cement and femur) has a total of 1223410 elements.

3. Result and discussion

3.1 Von Mises stresses

Prosthesis durability is closely related to the stresses distribution along the structure elements of the HTA, particularly in cement, which represents the weakest comparing the other elements. Moreover, the large stresses are intolerable by the patient and can lead to the loosening of the HTA. Figure 4 shows the distribution of the equivalent Von Mises stresses in orthopaedic cement for cement at ambient temperature and with varied temperatures, which the maximum stress is located on the proximal part of the cement, and reaches 18.5 MPa for cement with ambient temperature and for the other temperatures, these stresses show a certain progressive increase from 40°C to 90°C; for Von Mises stresses reaches the maximum value of 29.78MPa.

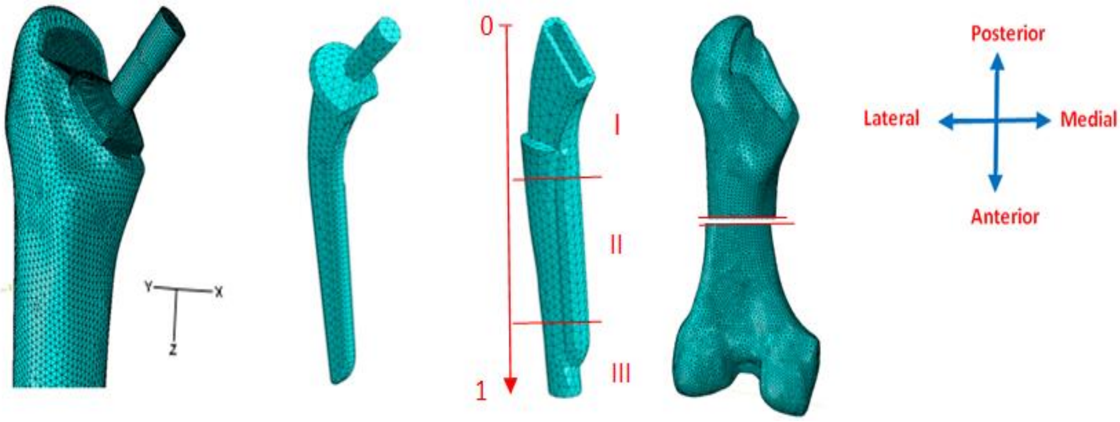

(a) (b) (c) (d)

Fig. 3 Finite element meshes of hip prosthesis components: a- Cemented hip stem, b-Osteal stem, c-Cement and (d) Femur bone, I: Proximal part, II: Median part and III: Distal part

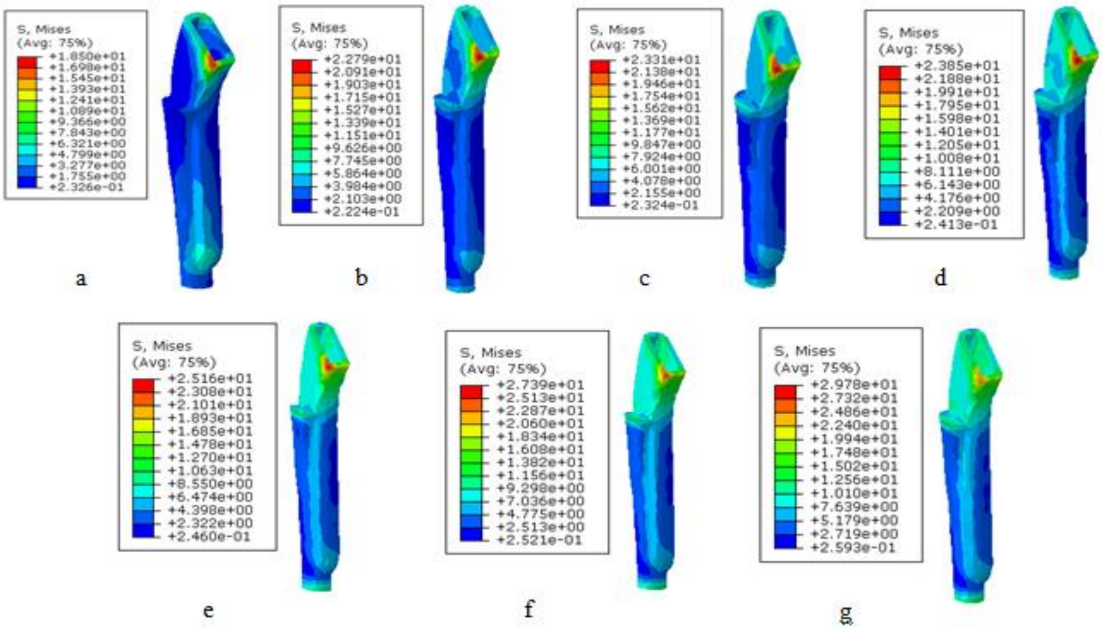

Fig. 4 Von Mises stress distribution on the cement with ambient temperature (a), with different temperatures [(b) 40°C, (c) 50°C,(d) 60°C,(e) 70°C,(f) 80°C and (g) 90°C]

Fig 5 shows the variation of the Von Mises stresses in the bone cement at different temperatures and with ambient temperature, solicited statically according to of the normalized distance to the implant cement interface in its lateral side. There are a relatively large concentration in the proximal part of the cement, it reaches around 26 MPa at a temperature of 90°C of the bone cement and begins to decrease until a stress of 21 MPa for a temperature of 40°C, this is due to the exothermic effect of the cement and its polymerization, without forgetting the static loading

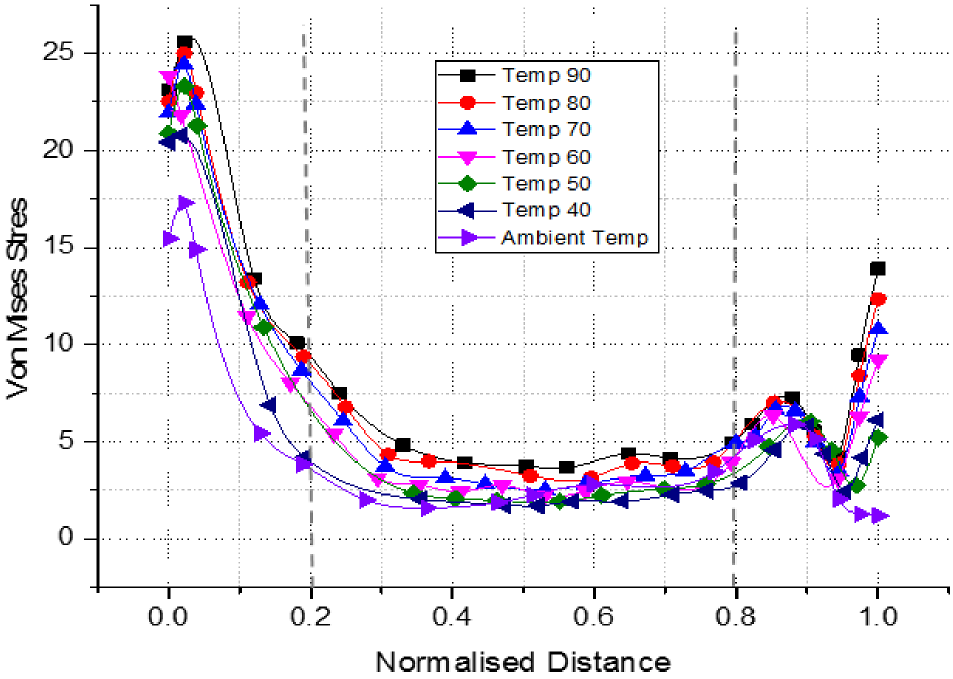

Fig. 5 Von Mises stresses in the cement mantle at the cement-implant interface on the lateral side with ambient temperature and with different temperatures versus the axial coordinate z

defined by the weight of the wearer of the total hip replacement. In the medial area, the Von Mises stresses do not exceed 08Mpa, while in the distal part; these stresses reach the 14 MPa, which causes no risk of rupture to the bone cement.

3.2 Normal stress (σx)

For the distribution of the normal stresses (σx), we note that this distribution is not uniform for all temperatures, and are distinguished for the cement with ambient temperature; the maximum stress reaches 12.57 MPa. For this case, the cement generates normal tensile stresses along this link and compressive stresses in the proximal area due to the adhesion of the implant and contraction of the cement during its cooling. For different representations at different temperatures, the cement is applied by normal compression stresses due to the polymerization of the cement and direct contact during insertion of the implant in order to ensure a good bond of the implant in the femoral cavity.

For the variation of the Normal stress distribution along the x-direction (σx) in the bone cement at different temperatures and with ambient temperature, as a function of the normalized distance to the implant cement interface in its lateral side, we note that in the proximal part, there is some tension stresses not exceeding 02.5 MPa for the cement at temperatures (40 °C, 50 °C and 60 °C) and with ambient temperature. For other temperatures, however and in the medial and distal regions, the cement is affected by the compressive stresses that exceed 05MPa and can reach 16MPa for the cement at 90 °C. This is due to the effect of the adhesion of bone cement on the implant and the exothermic reaction generated by the polymerization of the bone cement.

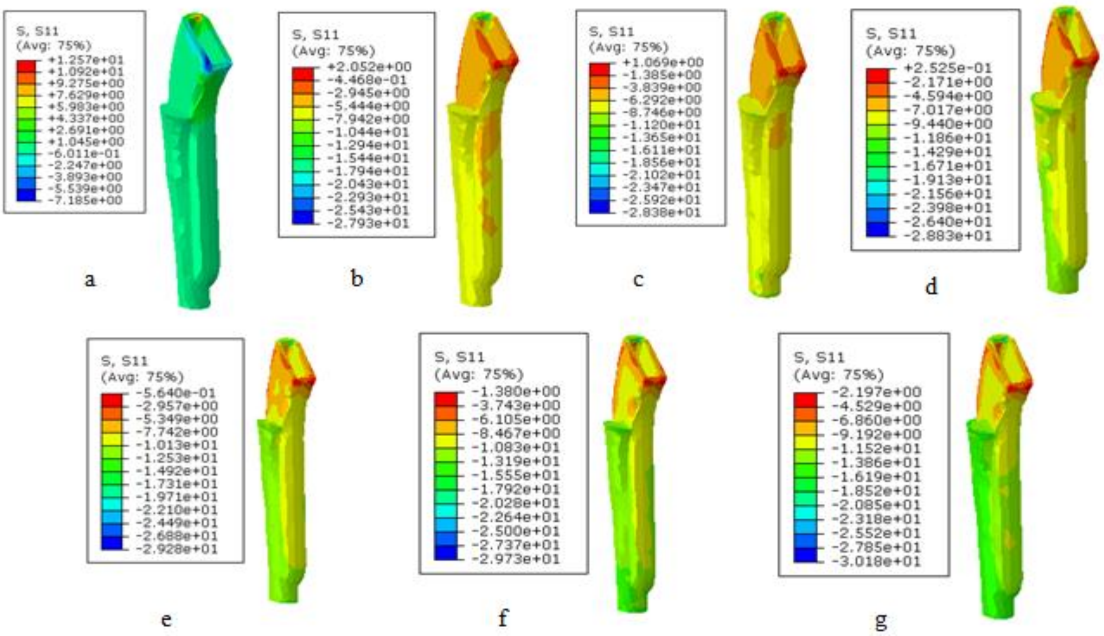

Fig. 6 Normal stress distribution according to x-direction (σx) on the cement with ambient temperature (a), and with different temperatures [(b) 40°C, (c) 50°C,(d) 60°C,(e) 70°C,(f) 80°C and (g) 90°C]

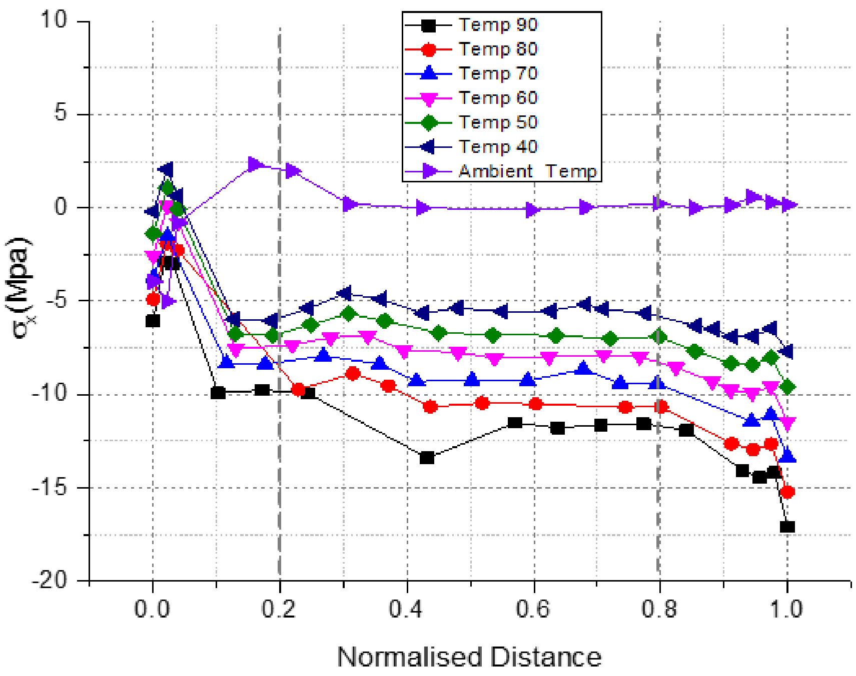

Fig. 7 Stresses according to x-direction (σx) in the cement mantle at the cement-implant interface on the lateral side with ambient temperature and with different temperatures versus the axial coordinate z

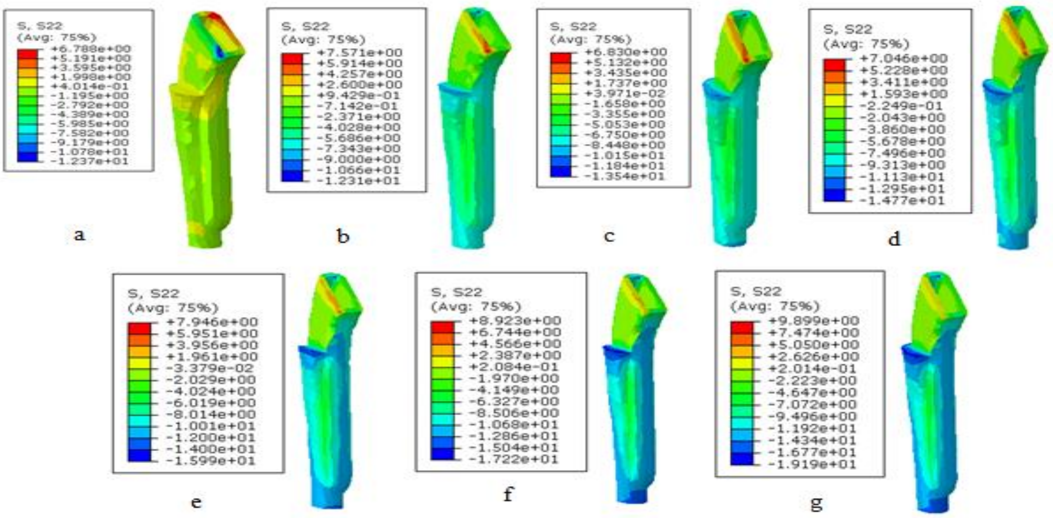

Fig. 8 Normal stress distribution according to y-direction (σy) on the cement with ambient temperature (a), and with different temperatures [(b) 40°C, (c) 50°C, (d) 60°C,(e) 70°C, (f) 80°C and (g) 90°C]

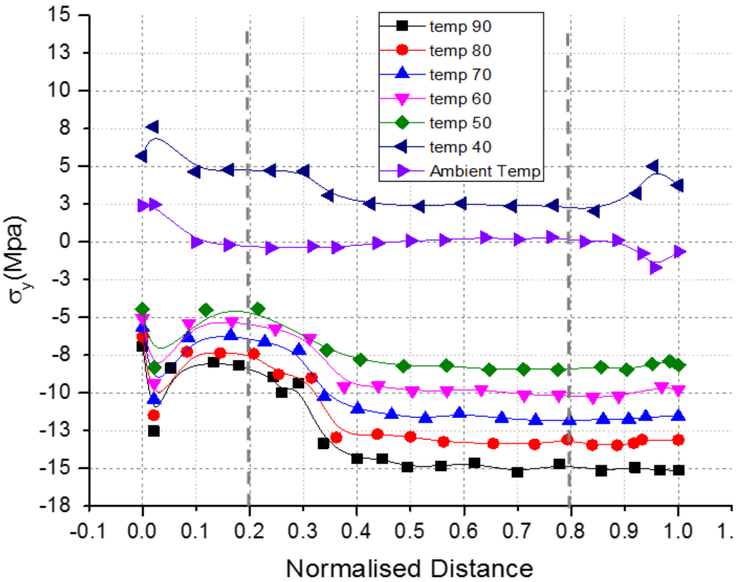

Fig. 9 Stresses according to y-direction (σy) in the cement mantle at the cement-implant interface on the lateral side with ambient temperature and with different temperatures versus the axial coordinate z

3.3 Normal stress (σy)

With regard to the distribution of normal stresses (σy) of the cement with ambient temperature and with different temperatures, the maximum induced stresses are localized in the proximal region of the cement, in particular in which the implant rests on its superior part, generating tensile stresses of 06.78 MPa for cement with ambient temperature and 09.89 MPa for temperature

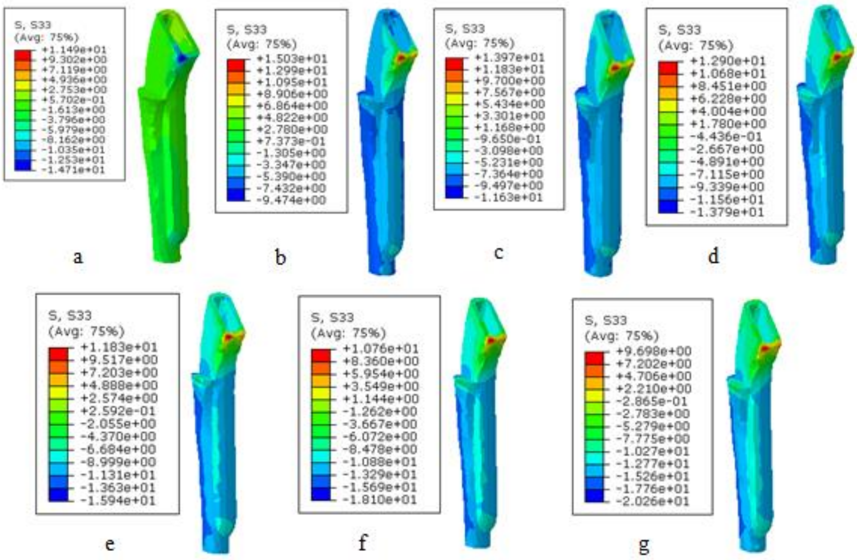

Fig. 10 Normal stress distribution according to z-direction (σz) on the cement with ambient temperature (a), and with different temperatures [(b) 40°C, (c) 50°C,(d) 60°C,(e) 70°C, (f) 80°C and (g) 90°C]

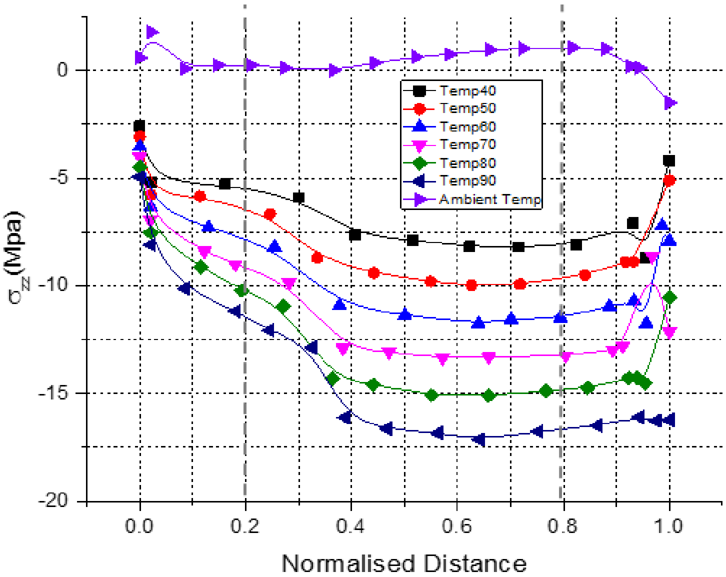

Fig. 11 Stresses according to z-direction (σz) in the cement mantle at the cement implant interface on the lateral side with ambient temperature and with different temperatures versus the axial coordinate z

of 90° C. In the medial and distal zone, the bone cement is affected by compression stresses; this is explained by the adhesion of the cement during its contraction on the implant and by its cooling creating tensile stresses and compression that present no risk of breaking the bone cement.

For the variation of the Normal stress (σy) in the bone cement at different temperatures and with ambient temperature, according to the normalized distance, is observed at the proximal part, the tensile stresses varying from 03.5MPa to 07.5MPa for the cement at 40 °C. For other temperatures, the cement is affected by compression stress lower 05MPa caused during the insertion of the implant at the start of the operation by the surgeon in the cement, and by the adhesion phenomenon of cement on the stem during its cooling.

3.4 Normal stress (σz)

Figure 10 shows that the normal stress distribution in the z-direction (σz) on the bone cement is not uniform, and the maximum stresses are localized in the proximal zone. This result in the transfer of the loading the weight of the wearer of the total hip prosthesis through the implant to the bone cement. However, the maximal stresses of cement with ambient temperature induced tensile stresses, which reach 11.49MPa, while for the cement at different temperatures; the normal stress reaches a maximum value of 15.03MPa for a temperature of 40°C. This stress gradually decreases from (40°C to 90°C) until a stress of 09.69MPa for 90°C. This decrease of the stress is explained by the polymerization of the cement and its contraction.

We note that the cement at ambient temperature is affected by tensile stress of 02.5 MPa on its proximal zone, whereas for other temperatures, the cement is affected by compressive stresses that vary between 2.5MPa to 5MPa in the proximal area and from 5MPa to 16MPa in the distal zone. This is due to the exothermic effect and by contraction, resulting in the cement inducing compressive stresses that force it to join the implant to ensure good bonding.

4. Conclusions

This study analyses the cement temperature effects during insertion of the implant by surgeons on the evolution of the induced stresses and make a comparison with the cement to ambient temperature, the results obtained lead to the following conclusion:

For the Von Mises stresses,there are a relatively large concentration in the proximal part of the cement, it reaches around 26 MPa at a temperature of 90°C and begins to decrease until a stress of 21 MPa for a temperature of 40°C; this is due to the exothermic effect of the cement and its polymerization.

For other normal stresses, the bone cement is affected by stresses of tension and compression due to the effect of polymerization and the contraction of the cement and by the phenomenon of adhesion.

In the cement mantle, the critical region is still predicted to be at the neck region of the hip total arthoplasty. The critical stress is much lower than the yield strength. Hence, the design of the prosthesis is believed to be safe for use.

The only disadvantage is the highest temperature of 90°C, in this case, during the operation, the patient would be anestesia, and the cement is cooled and solidifies in 10 minutes.

References

Perez, M.A, Grasa, J., Garcıa Aznar, J.M., Bea, J.A. and Doblare, M. (2006), “Probabilistic analysis of the influence of the bonding degree of the stem–cement interface in the performance of cemented hip prostheses”, *J. Biomech*., **39**(10), 1859-1872. https://doi.org/10.1016/j.jbiomech.2005.05.025.

Belkoff, S.M. and Molloy, S. (2003), “Temperature measurement during polymerization of polymethyl methacrylate cement used for vertebroplasty”, *Spine*, **28**(14), 1555-1559. https://doi.org/10.1097/01.BRS.0000076829.54235.9F.

Baroud, G., Samara, M. and Steffen, T. (2004), “Influence of mixing method on the cement temperature mixing time history and doughing time of three acrylic cements for vertebroplasty”, *J. Biomed. Mater. Res. B Appl. Biomater.*, **68**(1), 112-116. https://doi.org/10.1002/jbm.b.20009.

Ahmed, A.M., Burke, D.L. and Miller, J. (1982), “Transient and residual stresses and displacements in self-curing bone cement, Part 2: Thermoelastic analysis of the stem fixation system”, *J. Biomech. Eng.*, **104**(1), 28-37. https://doi.org/10.1115/1.3138300.

Ricker, A., Liu-Snyder, P. and Webster, T.J. (2008), “The influence of nano MgO and $BaSO_4$ particle size additives on properties of PMMA bone cement”, *J. Nanomedicine*, **3**(1), 125-132.

Iesaka, K., Jaffe, W.L. and Kummer, F.J. (2004), “Effects of the initial temperature of acrylic bone cement liquid mono mer on the properties of the stem-cement interface and cement polymerization”, *J. Biomedical Mater. Res. B Appl. Biomater.*, **68B**(2), 186-190. https://doi.org/10.1002/jbm.b.20020.

Li, C., Mason, J. and Yakimicki, D. (2004), “Thermal characterization of PMMA-based bone cement curing”, *J. Mater. Sci. Mater. Med.* **15**, 85-89. https://doi.org/10.1023/B:JMSM.0000010101.45352.d1.

Serbetci, K., Korkusuz, F. and Hasirci, N. (2004), “Thermal and mechanical properties of hydroxyapatite impregnated acrylic bone cements”, *Polym Test.*, **23**, 145-155. https://doi.org/10.1016/S0142-9418(03)00073-4.

Tunney, M.M., Brady, A.J., Buchanan, F., Newe, C. and Dunne, N.J. (2007), “Incorporation of chitosan in acrylic bone cement: effect on antibiotic release, bacterial biofilm formation and mechanical properties”, *the 21st European Conference on Biomaterials*, Brighton, United Kingdom, September.

Hong, R.Y., Fu, H.P., Zhang, Y.J., Liu, L., Wang, J., Li, H.Z. and Zheng, Y. (2007), “Surface-modified silica nanoparticles for reinforcement of PMMA”, *J. Appl. Polym. Sci.*, **105**(4), 2176-2184. https://doi.org/10.1002/app.26164.

Ricker, A., Liu-Snyder, P. and Webster, T.J. (2008), “The influence of nano MgO and $BaSO_4$ particle size additives on properties of PMMA bone cement”, *J. Nanomedicine*, **3**(1), 125-132.

Gillani, R., Ercan, B., Qiao, A. and Webster, T. (2010), “Nanofunctionalized zirconia and barium sulfate particles as bone cement additives”, *J. Nanomedicine*, **5**, 1-11.

Lai, P.L., Tai, C.L., Chu, I.M., Fu, T.S., Chen, L.H. and Chen, W.J. (2012), “Hypothermic manipulation of bone cement can extend the handling time during Vertebroplasty”, *BMC Musculoskeletal Disorders*, **13**(1), 198. https://doi.org/10.1186/1471-2474-13-198.

Tai, C.L., Chen, Y.L. and Chen, S.Y. (2014), “Temperature control of bone cement for enhancing applicability and safety in vertebroplasty”, *Appl. Mech. Mater.*, **684**, 395-399. https://doi.org/10.4028/www.scientific.net/AMM.684.395.

Whitehouse, M.R., Atwal, N.S., Pabbruwe, M., Blom, A.W. and Bannister, G.C. (2014), “Osteonecrosis with the use of polymethylmethacrylate cement for hip replacement: thermal-induced damage evidenced in vivo by decreased osteocyte viability”, *Eur. Cell Mater.*, **27**, 50-62. https://doi.org/10.22203/eCM.v027a05.

Baker, R., Whitehouse, M., Kilshaw, M., Pabbruwe, M., Spencer, R., Blom, A. and Bannister, G. (2011), “Maximum temperatures of 89°C recorded during the mechanical preparation of 35 femoral heads for resurfacing”, *Acta Orthop.*, **82**(6), 669-673. https://doi.org/10.3109/17453674.2011.636681.

Gundapaneni, D. and Goswami, T. (2014), “Thermal isotherms in PMMA and cell necrosis during total hip arthroplasty”, *J. Appl. Biomater. Funct. Mater.*, **12**(3), 193-202. https://doi.org/10.5301/jabfm.5000196.

Janssen, D., Srinivasan, P., Scheerlinck, T. and Verdonschot, N. (2012), “Effect of cementing technique and cement type on thermal necrosis in hip resurfacing arthroplasty--a numerical study”, *J. Orthop. Res.*, **30**(3), 364-370. https://doi.org/10.1002/jor.21512

Gergely, R.C., Toohey, K.S., Jones, M.E., Small, S.R. and Berend, M.E. (2016), “Towards the optimization of the preparation procedures of PMMA bone cement”, *J. Orthop. Res.*, **34**(6), 915-923. https://doi.org/10.1002/jor.23100.

Stolk, J., Janssen, D., Huiskes, R. and Verdonschot, N. (2007), “Finite element-based preclinical testing of cemented total hip implants”, *Clinical Orthopedics Related Res.*, **456,** 138-147.

https://doi.org/10.1097/BLO.0b013e31802ba491.

Benbarek, S., Sahli, A., Bouziane, M.M., Bachir Bouiadjra, B. and Serier, B. (2014), "Crack Length Estimation from the Damage Modelisation around a Cavityi in the Orthopedic Cement of the Total Hip Prosthesis", *Key Eng. Mater.*, **577-578**, 345-348. https://doi.org/10.4028/www.scientific.net/KEM.577-578.345.

Nuño, N. and Avanzolini, G. (2002), "Residual stresses at the stem-cement interface of an idealized cemented hip stem", *J. Biomech.*, **35**(6), 849-852. https://doi.org/10.1016/S0021-9290(02)00026-X.

WT